J.M. Hagedoorn, H. Greiner-Mai, L. Ballani, I. Wardinski & D. Stromeyer
Helmholtz Centre Potsdam
GFZ German Research Centre for Geosciences
Telegrafenberg, D-14473 Potsdam, Germany

Combined coupling torques for the electromagnetic and topographic core-mantle coupling and their influence on Earth's rotation

XY–374

DFG Research Unit 584
EGU General Assembly 2009, April 19 – 24, 2009

1 Introduction

We focus in this investigation on the consistent determination of the combined electromagnetic (EM) and topographic (TOP) core-mantle coupling torques. The combined coupling torque provides us the possibility to deduce equivalent excitation functions for the comparison with other contributions to the Earth's orientation parameters (EOPs), like atmospheric and oceanic angular momentum, on the decadal time scale.

2 Input models

2.1 Geomagnetic field model

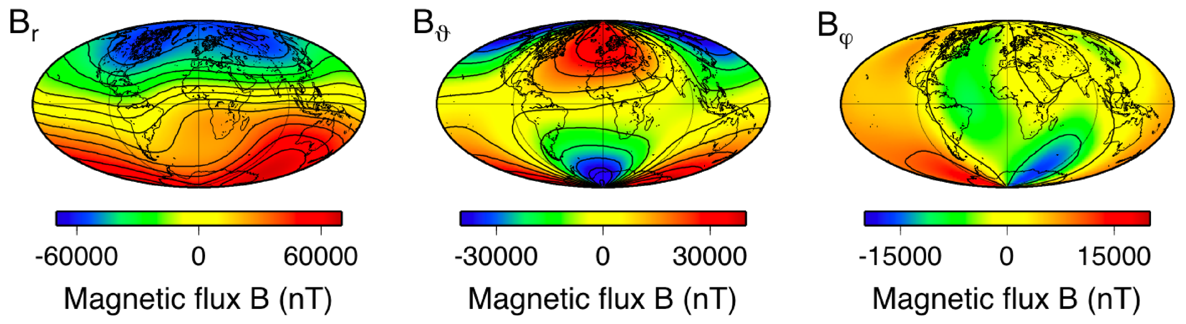

- Global geomagnetic field model C³FM *(Wardinski & Holme; 2006, JGR 111)* restricted to cut-off degree $j_{\max} = 8$. As an example are shown the components of $\boldsymbol{B}^{\mathsf{P}}$ at the Earth's surface for the year 1990
- Geomagnetic field decomposition into poloidal and toroidal parts by

$$\boldsymbol{B} = \boldsymbol{B}^{\mathsf{P}} + \boldsymbol{B}^{\mathsf{T}} = \mathrm{rot}\,\mathrm{rot}\,(\boldsymbol{r}S) + \mathrm{rot}\,(\boldsymbol{r}T)$$

- Observed geomagnetic field is a sole poloidal field $\boldsymbol{B}^{\mathsf{P}}$
- Spherical harmonic (SH) representation *(Varshalovich et al.; 1989, 'Quantum Theory of Angular Momentum')* of field quantities, e.g. for the toroidal scalar

$$T(r,\Omega,t) = \sum_{j=1}^{j\max}\sum_{m=-j}^{j} T_{jm}(r,t)Y_{jm}(\Omega)$$

2.2 Electrical conductivity models $\sigma_{\mathsf{M}}(r)$

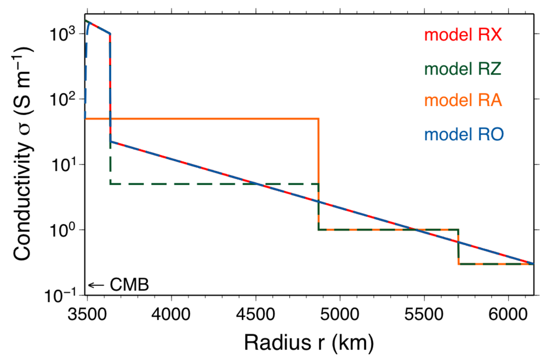

- Model RX with a conductance of $\sim 2\cdot 10^8$ S
- Model RZ with a conductance of $\sim 2\cdot 10^8$ S, reflects findings of EM induction studies (e.g. *Velímský et al.; 2006, GJI 166)*
- Model RA with a conductance of $\sim 0.7\cdot 10^8$ S
- Model RO with a conductance of $\sim 1.9\cdot 10^8$ S combined the model RX with findings of *Ono et al. (2005, EPSL 236)*,

2.3 CMB topography models

CMB model CD

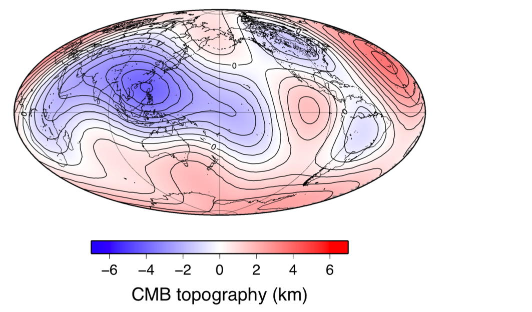

CMB model CS

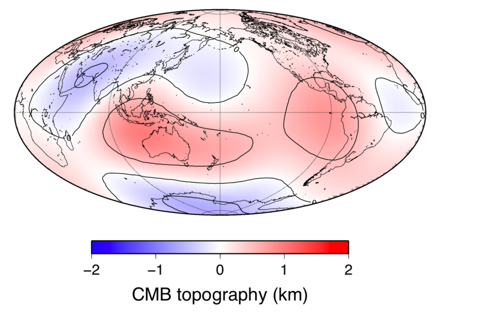

CMB model CM

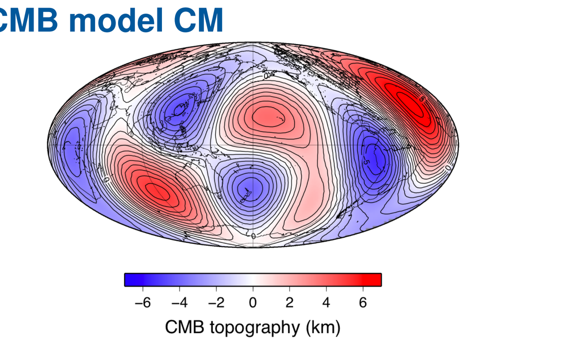

CMB model CT

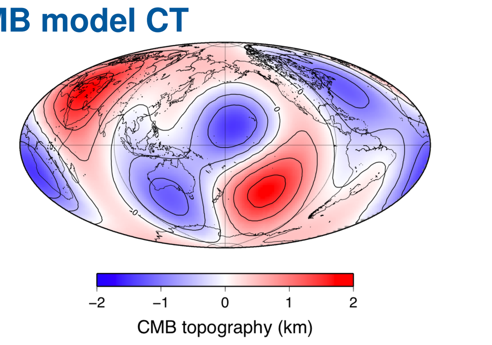

- All models show the undulation, h, of the CMB with respect to the hydrostatic ellipsoid according to *Denis et al. (1997, PEPI 99)*. In all calculations this additional deviation from the spherical reference surface is considered
- CMB model CD is taken from *Doornbos & Hilton (1989, JGR 94)*
- CMB model CM is taken from *Morelli & Dziewonski (1987, Nature 325)*
- CMB model CS is taken from *Sze & van der Hilst (2003, PEPI 135)*
- CMB model CT is taken from *Tanaka (2009, pers. comm.)*

3 Determination of input data at the CMB

3.1 Non-harmonic downward continuation (NHDC)

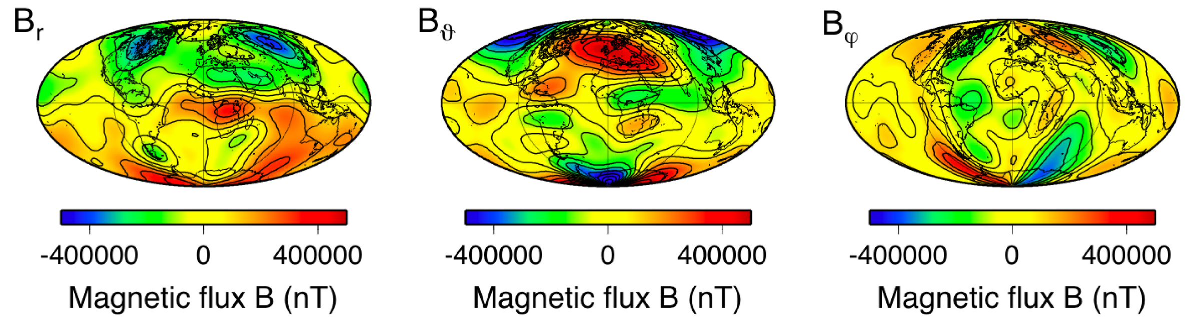

- Non-harmonic downward continuation (NHDC) of $\boldsymbol{B}^{\mathsf{P}}$ to the CMB according to *Ballani et al. (2002, GJI 149)* considering the different conductivity models
- Example above shows the components of $\boldsymbol{B}^{\mathsf{P}}$ at the CMB for the year 1990 considering the conductivity model RO by the NHDC

3.2 Fluid-flow inversion

Conductivity model RX

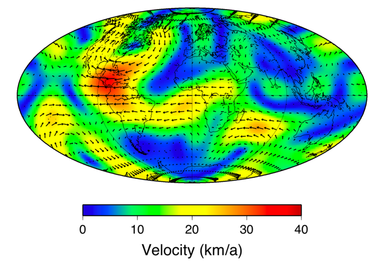

Conductivity model RO

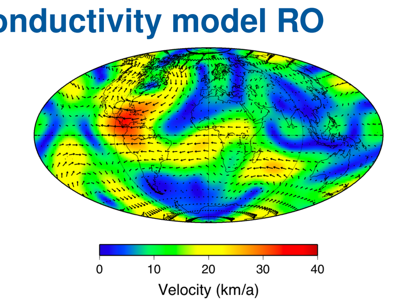

- Fluid-flow inversion according to *Wardinski (2005, GFZ STR 05/07)* assuming tangential geostrophy based on $\boldsymbol{B}^{\mathsf{P}}$ at the CMB determined by the NHDC
- Example for the calendar year 1993 considering the conductivity model RX and RA, respectively, and the related $\boldsymbol{B}^{\mathsf{P}}$ at the CMB
- Fluid-flow velocities differ only slightly, even for the two conductivity models RX and RA, where RA has only 37 % of the conductance of RX

3.3 Initial-boundary value problem (IBVP) for B^{T}

- Partial differential equation (PDE) for the field generating scalar $T_{jm}(r,t)$:

$$\frac{\partial^2}{\partial r^2}T_{jm}+\left[\frac{2}{r}-\frac{1}{\sigma_{\mathsf{M}}(r)}\frac{\partial}{\partial r}\sigma_{\mathsf{M}}(r)\right]\frac{\partial}{\partial r}T_{jm}-\left[\frac{j(j+1)}{r^2}+\frac{1}{r\sigma_{\mathsf{M}}(r)}\frac{\partial}{\partial r}\sigma_{\mathsf{M}}(r)\right]T_{jm}=\mu_0\sigma_{\mathsf{M}}(r)\frac{\partial}{\partial t}T_{jm}$$

- Boundary values ($|^-$ and $|^+$ indicate values below and above the boundary) of the first and third kind related to time-variable part of $T_{jm}(t)$:

$$T_{jm}(t)\,|^- = T_{jm}(t)\,|^+ = 0 \quad \text{at } R_\sigma \qquad \frac{\partial}{\partial r}(rT_{jm}(t))\,|^+ = -\mu_0\sigma_{\mathsf{M}}W_{jm}(t)\,|^- \quad \text{at } R_{\mathsf{CMB}}$$

where R_σ is the boundary between the insulating and the conducting mantle and R_{CMB} is the boundary between the lower mantle and the liquid outer core
- Determination of the boundary value, W_{jm}, in SH representation is based on the poloidal geomagnetic field, S_{jm}, and the surface fluid-flow velocity of the outer core, P_{st} and Q_{st} *(see also Hagedoorn & Greiner-Mai; 2008, GFZ STR 08/06)*

$$W_{jm} = \frac{-1}{j(j+1)}\sum_{klst}k(k+1)S_{kl}(t)\left[\mathbf{L}^{jm}_{klst}\,P_{st}(t) - \mathbf{K}^{jm}_{klst}\,Q_{st}(t)\right]$$

$\mathbf{K}^{jm}_{klst}$ and $\mathbf{L}^{jm}_{klst}$ are combinations of Clebsch-Gordan coefficients
- Solving the IBVP by finite-difference schema, where the quadratic approximation in space and time is realized by a Crank-Nicolson approach

4 Coupling torques

4.1 EM coupling torques

Poloidal torques *(see also Hagedoorn & Greiner-Mai; 2008, GFZ STR 08/06)*

$$L^{\mathsf{P}}_z = \frac{R_{\mathsf{CMB}}}{\mu_0}\int_\Omega \Delta_\Omega S\frac{\partial^2}{\partial\varphi\partial r}(rS)\,d\Omega \quad \text{where} \quad \Delta_\Omega = \left[\frac{1}{\sin\vartheta}\frac{\partial}{\partial\vartheta}\left(\sin\vartheta\frac{\partial}{\partial\vartheta}\right)+\frac{1}{\sin^2\vartheta}\frac{\partial^2}{\partial\varphi^2}\right]$$

$$L^{\mathsf{P}} = L^{\mathsf{P}}_x + iL^{\mathsf{P}}_y = -\frac{1}{\mu_0}\int_\Omega(\Delta_\Omega S)e^{i\varphi}\left[\cot\vartheta\frac{\partial^2}{\partial r\partial\varphi}(rS) - i\frac{\partial^2}{\partial r\partial\vartheta}(rS)\right]r\,d\Omega$$

Toroidal torques

$$L^{\mathsf{T}}_z = -\frac{R^2_{\mathsf{CMB}}}{\mu_0}\int_\Omega \Delta_\Omega S\sin\vartheta\frac{\partial}{\partial\vartheta}T\,d\Omega$$

$$L^{\mathsf{T}} = L^{\mathsf{T}}_x + iL^{\mathsf{T}}_y = \frac{1}{\mu_0}\int_\Omega(\Delta_\Omega S)e^{i\varphi}\left[\frac{i}{\sin\vartheta}\frac{\partial}{\partial\varphi}T + \cos\vartheta\frac{\partial}{\partial\vartheta}T\right]r^2\,d\Omega$$

4.2 TOP coupling torques

Poloidal torques *(see also Greiner-Mai & Hagedoorn; 2008, GFZ STR 08/11)*

$$L^{\mathsf{P}}_z = -2\bar{\rho}\omega_0 R^3_{\mathsf{CMB}}\int_\Omega h(\Omega)\,\sin\vartheta\frac{\partial}{\partial\vartheta}P\,\cos\vartheta\,d\Omega$$

$$L^{\mathsf{P}} = L^{\mathsf{P}}_x + iL^{\mathsf{P}}_y = 2\bar{\rho}\omega_0 R^3_{\mathsf{CMB}}\int_\Omega h(\Omega)\left[\cos\vartheta\frac{\partial}{\partial\vartheta}P + i\frac{1}{\sin\vartheta}\frac{\partial}{\partial\varphi}P\right]e^{i\varphi}\cos\vartheta\,d\Omega$$

Toroidal torques

$$L^{\mathsf{T}}_z = -2\bar{\rho}\omega_0 R^3_{\mathsf{CMB}}\int_\Omega h(\Omega)\frac{\partial}{\partial\varphi}Q\,\cos\vartheta\,d\Omega$$

$$L^{\mathsf{T}} = L^{\mathsf{T}}_x + iL^{\mathsf{T}}_y = 2\bar{\rho}\omega_0 R^3_{\mathsf{CMB}}\int_\Omega h(\Omega)\left[\cot\vartheta\frac{\partial}{\partial\varphi}Q - i\frac{\partial}{\partial\vartheta}Q\right]e^{i\varphi}\cos\vartheta\,d\Omega$$

S/T: field-generating scalar of $\boldsymbol{B}^{\mathsf{P}}/\boldsymbol{B}^{\mathsf{T}}$ $\quad\mu_0$: permeability of the vacuum
P/Q: representing scalars of fluid flow velocity $\boldsymbol{u}$ $\quad\bar{\rho}$: mean mass density of the fluid core
$h(\Omega)$: CMB topography with resp. to reference sphere $\quad\omega_0$: mean daily frequency

5 Equivalent excitation functions

- Basic assumption: Earth consists of a two component system of mantle and core, where the related EM and TOP coupling torques act on the CMB
- For the mantle the following linearised Liouville equations in the complex notation ($L = L_x + i\,L_y$, $m = m_x + i\,m_y$, $\chi = \chi_x + i\,\chi_y$) are valid:

$$m(t) + \frac{i}{\lambda}\dot{m}(t) = \frac{iL(t)}{\omega_0^2(\boldsymbol{C}_{\mathsf{M}} - \boldsymbol{A}_{\mathsf{M}})} + \chi(t) - \frac{i}{\omega_0}\dot{\chi}(t)$$

$$\dot{m}_z(t) = -\left(\frac{-L_z(t)}{\omega_0\boldsymbol{C}_{\mathsf{M}}} + \dot{\chi}_z(t)\right)$$

$\boldsymbol{C}_{\mathsf{M}}/\boldsymbol{A}_{\mathsf{M}}$: polar / equatorial moment of inertia of the Earth's mantle $\quad\omega_0$: mean daily frequency

- Equivalent excitation functions are defined related to the equations above by the following integrals:

$$\chi(t) = e^{-i\omega_0(t-t_0)}\left[\chi_0 + \int_{t_0}^{t}\frac{-L(\tau)}{\omega_0(\boldsymbol{C}_{\mathsf{M}} - \boldsymbol{A}_{\mathsf{M}})}e^{i\omega_0(\tau-t_0)}d\tau\right]$$

$$\chi_z(t) = \int_{t_0}^{t}\frac{-L_z(\tau)}{\omega_0\boldsymbol{C}_{\mathsf{M}}}d\tau$$

- For our investigation on the decadal time scale, it is possible to average out the mean daily freuquency of the Earth's rotation in the x- and y-component of the equivalent excitation functions
- Dimensionless variation of the Earth's rotation, given by m and m_z are expressed as polar motion (ΔX,ΔY) and variation of length-of-day (ΔLOD)

6 Results of the numerical calculations

6.1 Resulting coupling torques

EM coupling torques ΔL^{EM}

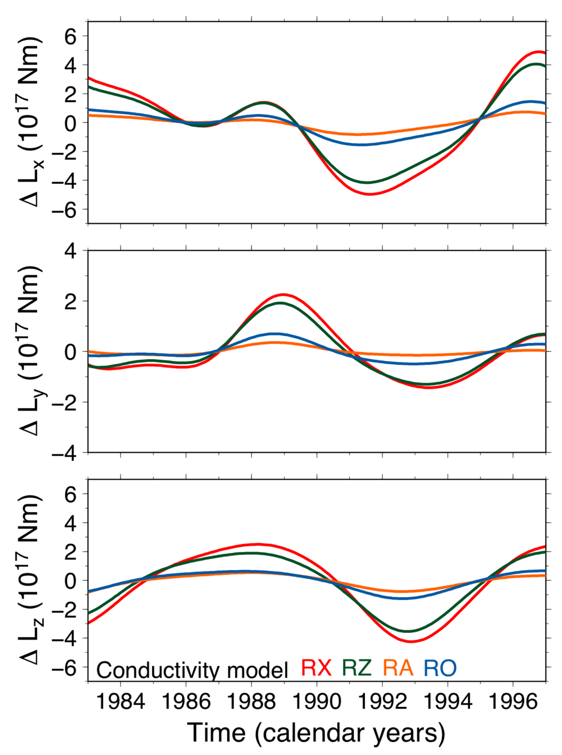

TOP coupling torques ΔL^{TOP}

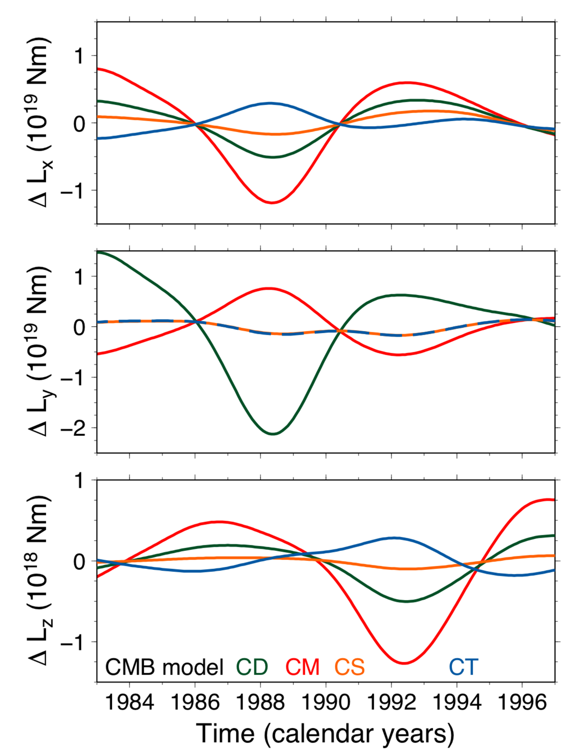

For comparison all resulting torques $\boldsymbol{L}$ are reduced for their linear trends. The residual variations are denoted by $\Delta\boldsymbol{L}$.

6.2 Equivalent excitation functions

EM coupling equivalent χ^{EM}

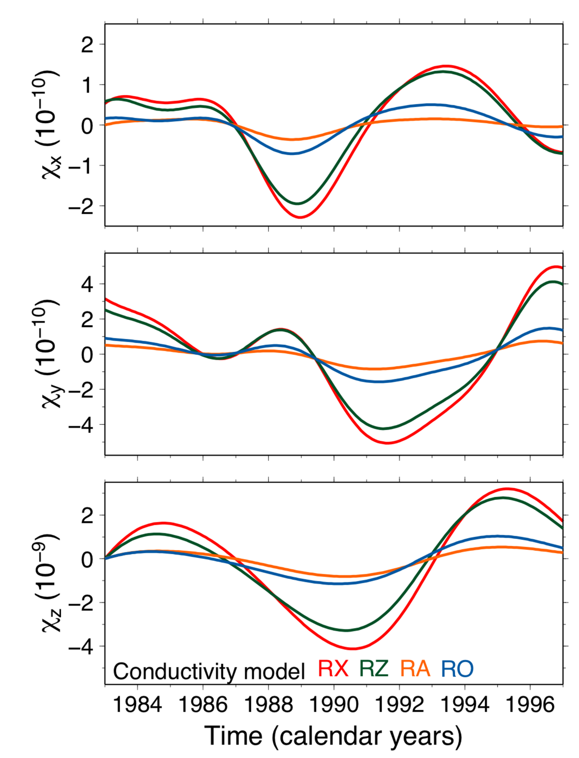

TOP coupling equivalent χ^{TOP}

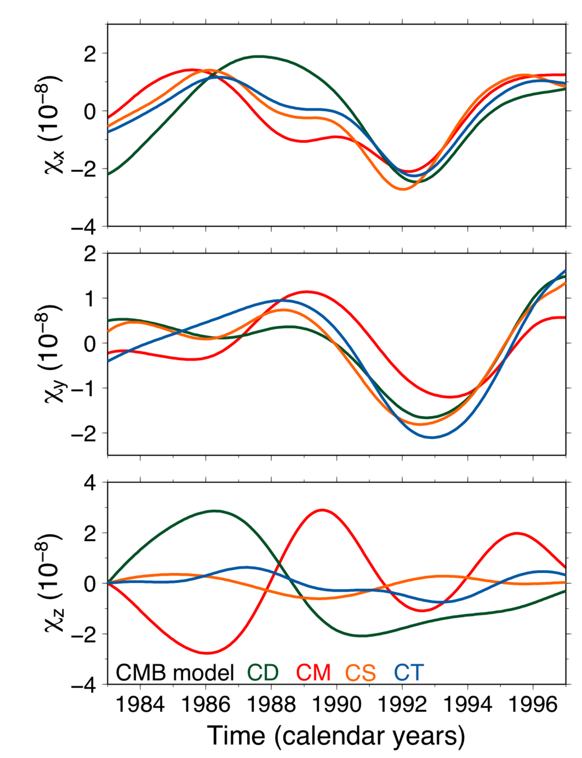

For comparison all resulting equivalent excitation functions are reduced for their linear trends.

6.3 Comparison with observed EOPs

Modelled variation of EOPs (ΔX,ΔY,ΔLOD)

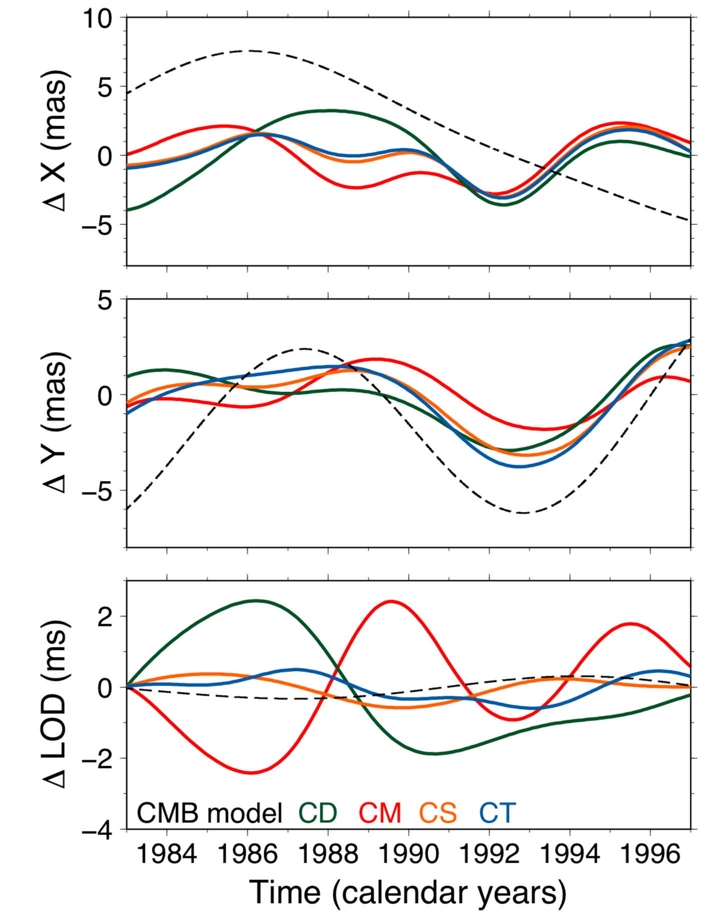

Polar motion (ΔX,ΔY) and variation of length-of-day (ΔLOD). Black, dashed lines show the observed decadal variation of EOPs.

- Conductivity model RO is used for all calculations
- Forward calculations of EOPs based on linearised Liouville equations and following excitations:
  - EM coupling χ^{EM}
  - TOP coupling χ^{TOP}
  - atmospheric angular momentum (AAM, provided by OMCT model)
  - oceanic angular momentum (OAM, provided by OMCT model)
- The dashed black line: six-years bandpass filtered EOP time series from the IERS (EOP C04)
- Colored lines: combined modelled EOPs for different CMB topography models

7 Discussion & Conclusion

- EM coupling torques have an order of magnitude of $\sim 10^{17}$ Nm in all components, which is not sufficient for polar motion excitation
- TOP coupling torques
  - different CMB topography models lead to different time behavior and amplitudes for all components of the topographic coupling torque
  - z-component is in the order of 10^{18} Nm where as x- and y-components are in the order of 10^{19} Nm
- Conclusion & outlook
  - Comparison between observed and modelled ΔLOD allows to exclude certain CMB topography models (CD, CM), because their contributions to ΔLOD contradict the observations
  - Comparison between observed and modelled polar motion show similar amplitudes but highlights the need for longer time series for forward modelling of EOPs
  - Considering combined coupling torques leads in all three components to results in the same order of magnitude as the observed EOPs
  - Differences between observed and modelled EOPs may be due to the neglect of further coupling processes like gravitational core-mantle coupling

E-mail jan@gfz-potsdam.de